Photosynthetic reaction center-based biophotovoltaics

Friebe, Vincent M.; Frese, Raoul N.

published in
CURRENT OPINION IN ELECTROCHEMISTRY
2017

DOI (link to publisher)
10.1016/j.coelec.2017.08.001

document version
Publisher's PDF, also known as Version of record

Available online at www.sciencedirect.com
ScienceDirect
Current Opinion in Electrochemistry

Review Article

Photosynthetic reaction center-based biophotovoltaics

Vincent M. Friebe and Raoul N. Frese*

Photosynthesis is the principal solar energy conversion process on Earth, but is low in overall efficiency due to numerous steps necessary to fix carbon. Tapping into the high-efficiency components which drive photosynthesis, known as reaction centers, offers a route to efficiently capture solar energy. This may be achieved by direct integration of reaction centers onto electrode materials in order to extract the high potential electrons and produce electricity or fuels. This review describes the various strategies and current benchmark configurations of Photosystem-I, Photosystem-II and bacterial reaction center-based biophotoelectrodes.

Address
Department of Physics and Astronomy, LaserLaB Amsterdam, VU University Amsterdam, De Boelelaan 1081, Amsterdam 1081 HV, The Netherlands

*Corresponding author: Frese, Raoul N. (r.n.frese@vu.nl)

Current Opinion in Electrochemistry 2017, **5**:126–134

This review comes from a themed issue on **Bioelectrochemistry**

Edited by **Nicolas, Wolfgang**

For a complete overview see the Issue and the Editorial

Available online 8 August 2017

http://dx.doi.org/10.1016/j.coelec.2017.08.001

Photosynthesis for device application

Solar energy is the most abundant energy source, striking Earth's surface at a rate of ~120,000 TW [1,2]. Photosynthesis, the principal solar energy conversion process on the planet, captures and stores solar energy as biomass at a rate of ~120 TW, or more than six times our current rate of energy consumption (~18 TW) [1,2]. While utilizing this biomass to meet our energy demands seems attractive, a number of challenges render this economically and environmentally unfeasible [3,4]. In large part, this is due to the low efficiency in which solar energy is converted into biomass, with crop plants obtaining only a few percent efficiency at best [3,5].

Photosynthesis begins with the absorption of light by a pigment-protein complex, forming excitation energy which drives primary charge separation in the photochemical reaction center (RC) (Figure 1). This sets in motion a series of down-hill redox reactions which produce ATP and NADPH. This chemical potential energy is used in subsequent enzyme reactions to fix CO_2in the form of carbohydrates. Losses in power conversion efficiency occur at each of these steps, particularly after intra-protein charge separation in the RC [6], driving the interest to the extract high potential electrons directly from the RC.

While photosynthesis occurs in species separated by billions of years of evolution: bacteria, algae and plants, the general functional and structural layout of their RCs are very similar. An RC consists of a protein scaffold that binds chromophores such as chlorophylls and carotenoids, which act as functional light-harvesting or electron transfer components. Light-driven charge separation is initiated at a specific group of chlorophyll-like molecules named the special pair (indicated by P and wavelength of maximum absorption) and the electron is transferred within a few picoseconds to a nearby pheophytin molecule [7]. Some evolutionary adjustments have been made regarding the transition energy and the redox potentials of the photocatalytic sites, for example, PS-II of plants and green algae is sufficiently oxidizing enough to extract electrons from water. As a result of these adjustments, the intraprotein power conversion efficiencies (η_{RC}) of bacterial RCs (BRC), photosystem-I and photosystem-II (PS-I and PS-II) are 32%, 57%, and 59%, respectively. These are calculated from the values in Table 1 using the following equation:

$$\eta_{RC} = \frac{T}{P^*}$$

where T is the terminal cofactor energy relative to the special pair ground state (Δ eV vs. P) and P^* is the special pair HOMO–LUMO gap (Δ eV). This calculation assumes the quantum efficiency of charge separation is 100%.

All types of RCs in nature are surrounded by species-specific light-harvesting complexes (LHC's) that absorb light and transfer excited state energy towards the RC. Note that RC–LHC systems are generally indicated with names to reflect the type of LHC; such as RC–LH1 for bacterial species. For simplicity, we generally use the abbreviation RC in the text for all preparations.

Since the stimulating light is typically not a single wavelength, but rather the solar spectrum above the band gap, spectral losses are taken into account by the ultimate

Figure 1

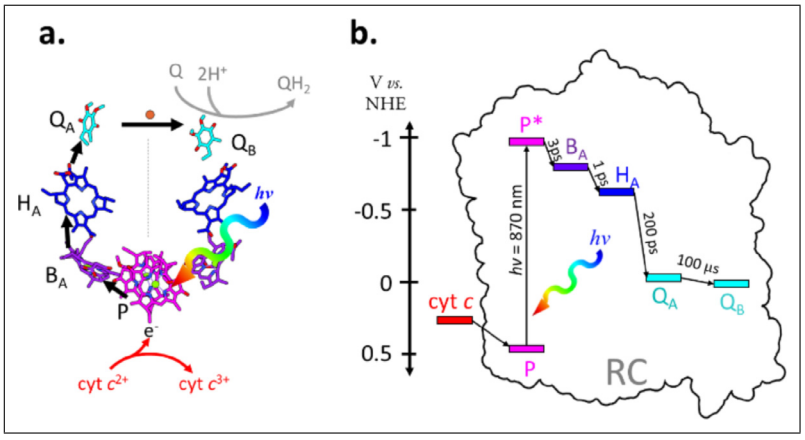

The energetics and mechanism of unidirectional charge separation in the bacterial reaction center. a) The cofactors within the RC involved in charge separation with only those of the A-branch listed. The special pair (P) in magenta, bacteriochlorophyll (B_A) in purple, bacteriopheophytin (H_A) in blue and ubiquinones (Q_A) and (Q_B) in cyan. External electron donors and acceptors cytochrome *c* and ubiquinone are shown in red and gray arrows, respectively. The rotational axis of symmetry is shown in dotted lines b) electron transfer with formal potentials of the cofactors as well as electron transfer lifetimes. Structural outline of the BRC protein complex indicated by the black outline, height is approximately 6 nm.

Table 1

Estimated redox midpoint potentials (E_m) and ultimate efficiencies.

Reaction center *R. sph.*	E_m (mV vs. NHE)	HOMO–LUMO gap (Δ eV vs. P)	Ultimate efficiency (%)
$P870^+/P870$	+450 mV [8]	–	–
P870*	−975 mV[a]	1.43 eV	45.4%[b]
Q_B/Q_B^-	−10 mV [9,10]	0.46 eV	14.6%
Photosystem I			
$P700^+/P700$	+450 mV [11]	-	–
P700*	−1320 mV [11]	1.77 eV	36.2%
F_B/F_B^-	−560 mV [12]	1.01 eV	20.7%
Photosystem II			
$P680^+/P680$	+1125 mV	-	–
P680*	−705 mV [13]	1.82 eV	34.6%
Q_B/Q_B^-	+40 mV [14]	1.08 eV	20.4%
Silicon		1.11 eV	48.6%

[a] Estimated using E_m P_{870}^+/P_{870} -1.425 V (870 nm = 1.425 eV).

efficiency (η_U) depicted in Figure 2 for BRCs and PS-I [15]. The η_U is part of the Shockley Queisser method devised to calculate the limits of solar energy conversion and is defined as the maximum power conversion efficiency of a single junction (single photosystem) material from spectral losses. It assumes that the quantum efficiency is one at all wavelengths above the band gap, photons with higher energy relax down to the band gap energy, the only mechanism of loss is radiative recombination, and that photons below the band gap are not absorbed [15]. It may be calculated as a function of the band gap frequency (v_g, s^{-1}) using the following equation:

$$\eta_U(v_g) = \frac{h\, v_g\, N_p}{P_{in}}$$

where h is Planck's constant (6.626×10^{-34} J s), N_p is the number of incident photons per defined area above the band gap energy, and $P_{in}$is the cumulative solar irradiance ($W\,m^{-2}$) [16]. Using the AM 1.5 G solar irradiance and the BRC P870 band gap of 1.43 eV we determined the $\eta_{\mu\ BRC} = 45.4\%$. To extend the calculation to the BRC

Figure 2

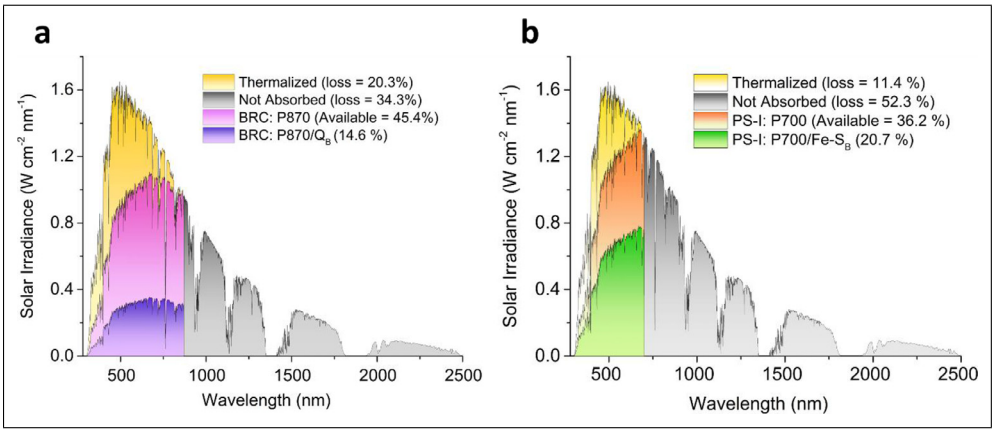

Reaction center ultimate efficiencies. *R. sphaeroides* BRC and Photosystem-I efficiency losses from transmission (grey), thermalization (yellow), with available remaining energy at the special pair (magenta and orange) and after charge separation (purple and green). Efficiencies and losses are indicated in parentheses in the legend and corresponding colored areas are to scale. PS-II is not shown here but has similar ultimate efficiencies to PS-I (see Table 1).

terminal cofactor (Q_B) the η_U (45.4%) is multiplied by the η_{RC} (32%) to obtain a 14.6% ultimate efficiency after charge separation (Q_B^-/P^+). The η_U calculation is extended to reveal PS-1 and PS-II have a η_U of 20.7% and 20.6% after charge separation (Table 1). Our η_U calculations are in good agreement with Mirvakili *et al.* [17] but differ slightly due to our use of the AM 1.5 G solar irradiance spectrum rather than a 6000 K blackbody irradiance and variations in the reported cofactor redox potentials [9,10].

By integrating the area of the solar irradiance curve below the band gap of the RC, we calculated that 34% and 52% of solar irradiation is not absorbed by BRCs and PS-I complexes, respectively (Figure 2, gray). Of the fraction absorbed, 20.3 % is lost as heat due to thermal relaxation of the excitation energy down to the fixed-band gap energy of P870 in BRCs, while only 11.4% is lost in PS-I due to the larger band gap (Figure 2, yellow). In retrospect, an optimal RC tuned to the solar irradiance would have a larger intraprotein potential energy, similar to PS-I, but a larger spectral range extending further into the infrared, similar to the BRC.

Progress and strategies in biophotovoltaics

Incorporating the high power conversion efficiencies of RCs into devices has gained a significant amount of interest in recent years [18,19]. This has resulted in significant improvement in biophotovoltaic performances, with densities in the microampere per cm^{-2} range becoming the norm [20••–23•] and some even reaching the milliampere range [24•,25]. Key developments in biophotovoltaic progress utilizing all types of RCs are depicted in Figure 3. Progress is measured in photocurrents densities (J_{photo}) rather than power conversion efficiencies, as most of the reported values are from half-cell configurations with an applied bias potential. The various methodologies used to immobilize RCs on electrodes have been recently reviewed for BRCs [18], PS-I [26], PS-II in [27], and collectively for all RCs types [19,28]. A recent book chapter by Plumeré and Nowaczyk provides an excellent guideline for biophotoelectrochemistry and is indispensable for navigating the following text [29•].

Protein immobilization

Perhaps the most common and simple method to construct biophotoelectrodes is electrode immersion in a solution containing the solubilized RCs. Modulation of the substrate composition, architecture, or surface chemistry is typically employed to facilitate protein-electrode adsorption, as it is more accessible than modulating the complex protein surface itself. Nevertheless, there are also several instances of engineering the RC itself for electrode binding. For example, PS-I has been engineered to bind metal oxides [30,31], and histidine-tags have been added on both BRCs and PS-II for binding Ni-NTA functionalized electrodes [32,33].

A common method for interfacing proteins with metal electrodes is surface functionalization with a self-assembled monolayer (SAM). A SAM typically consists of an alkanethiol on gold [32] and silver [56] electrodes, or silanes and phosphonates on indium tin oxide (ITO) [36,45]. Numerous groups including Kong *et al.* [54], Nango *et al.* [37], and Trammell & Lebedev [50] have constructed metal-SAM electrodes. Relatively low J_{photo} of tens of nanoamperes were reported due to slow heterogeneous electron transfer from the electrode the RC. This is a result of the additional tunneling barrier imposed by both the SAM spacer (e.g. ~1 nm for a 6-carbon SAM)

Figure 3

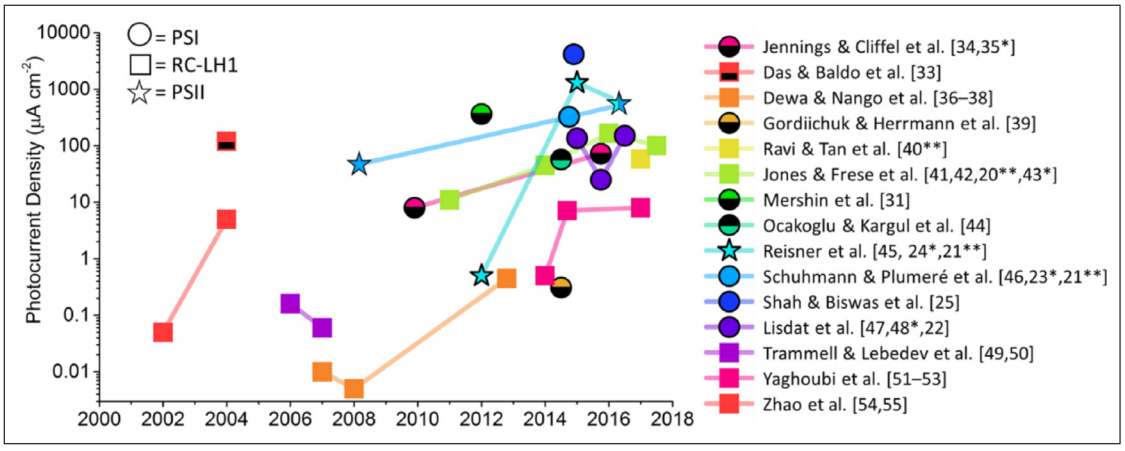

Recent progress in biophotovoltaics. Achievements by various laboratories are indicated by maximum photocurrents (log scale) and year of report. PSI-based electrodes are indicated by circles, BRC-based electrodes in squares, PS-II is indicated by stars, and two-electrode power generating configurations are filled half-black. Ref. [21••] is a collaboration between the two groups indicated. References in square brackets are in chronological order consistent with data points. The references cited in this figure are [20••,21••,22,23•,24•,25], [33,34,35•,36–39,40••,41,42,43•,44–47,48•,49–55].

[37] and the protein matrix of the RC which is ~0.7 nm for the donor side and 2.4 nm from the ubiquinone acceptor side [49] (SI).

Long tunneling gaps may be bridged by electron relays or immobilized electron transfer mediators. This was pioneered by Lebedev *et al.* [49] with the addition of the natural RC electron donor, cytochrome *c* (cyt *c*), on a functionalized gold electrode, leading to a 40-fold increase in J_{photo} up to 160 nA cm^{-2}. Yaghoubi *et al.* [51] further improved protein loading from 4 pmol cm^{-2} to 6 pmol cm^{-2} and J_{photo} up to ~500 nA cm^{-2} by substituting the Ni-NTA terminated SAM for a shorter hydroxyl-terminated SAM. The tunneling barrier can be further minimized by removing the SAM entirely and directly immobilizing RCs and cyt *c* onto bare gold electrodes. This was demonstrated by Hollander *et al.* [41] who obtained a J_{photo} of ~ 11 μA cm^{-2} ($\lambda = 870$ nm at 100 mW cm^{-2}).

Further improvements in photocurrent can be obtained by increasing the RC packing density and controlling the RC orientation, which enables favorable electron transfer from an electrode to either the acceptor or donor side of the RC. One such technique, the Langmuir–Blodgett film deposition method, exploits the innate amphiphilic nature of certain RCs to orient the complexes donor-side-up on an air–water interface. Deposition of an oriented and densely packed BRC film on an electrode is described in Kamran *et al.* [57] and resulted in a J_{photo} of 45 μA cm^{-2} ($\lambda = 880$ nm at 23 mW cm^{-2}). This represented a milestone for monolayer-based systems, as the internal quantum efficiency (IQE, electrons per absorbed photon) approached 32%, meaning one in every three RC excitations resulted in an electron transfer from the electrode.

The turnover over frequency (TOF) may be extrapolated from the photocurrent ($J = 45$ μA cm^{-2}) and protein loading ($\Gamma_{RC\text{-}LH1} = 1.1$ pmol cm^{-2}) reported by Kamran *et al.* using the following equation:

$$TOF = \frac{J}{F\,\Gamma_{RC-LH1}}$$

where F is the Faraday constant (96,485 C mol^{-1}). This revealed an RC-LH1 TOF of ~400 e$^-$ s^{-1}, the highest for a BRC-based system to date [42]. The TOF is essential in revealing not only the rate but also the extent to which the RCs that are immobilized are utilized (e.g. relative to maximum turnover [29•]) and should be reported for biophotoelectrode comparison. Regardless of the high TOF reported by Kamran *et al.*, the low BRC loading lead to a correspondingly small external quantum efficiency (EQE, electrons per incident photon) of 0.28%, prompting the departure from flat surfaces to larger surface area structures for higher BRC loading discussed below.

Another strategy to orient and densely pack RCs exploits the high affinity of polyhistidines to bind Ni-NTA functionalized electrodes. However, photocurrent densities on these substrates typically reside in the nanoampere range [32,49,38], with two exceptions in the microampere range [33,58]. For a direct comparison, see the 10-fold larger photocurrent response of PS-II randomly oriented within a redox polymer on gold relative to His-tag immobilization on Ni-NTA functionalized gold [46].

For device application, large surface area electrodes are necessary to increase the RC loading and overall performance. Friebe *et al.* [20••] showed that the transition

from a planar silver substrate to a mesoporous rough silver electrode resulted in J_{photo} enhancements of approximately six fold, from ~30 μA cm^{-2} to 166 μA cm^{-2}, and a TOF increase from 57 to 142 e$^-$ s^{-1} under 1-sun illumination. Similarly, Kato *et al.* [59] immobilized PS-II on mesoporous ITO increasing PS-II loading 26-fold relative to an ideal monolayer, totaling 19 pmol cm^{-2}. This resulted in a J_{photo} of ~1.6 μA cm^{-2} by direct electron transfer (DET), and 22 μA cm^{-2} by mediated electron transfer (MET) via the addition of 2,6-dimethylbenzoquinone (DCBQ) (λ = 685 nm at 10 mW cm^{-2}). Subsequent work focused on further increasing the effective surface area of the mesoporous ITO, utilizing macroporous polystyrene spacers (0.75 μm) to obtain hierarchical inverse opal mesoporous ITO electrodes. This increased the loading of PS-II up to 1020 pmol cm^{-2} [24•] and resulted in a J_{photo} of ~20 μA cm^{-2} by DET. The addition of the mediator DCBQ boosted the peak current up to 1300 μA cm^{-2} (λ = 680 nm at 10 mW cm^{-2}), the highest value to date for a PSII-based system. However, the reported PS-II TOF of ~52 e$^-$ s^{-1} is only a fraction of the previously reported 500 e$^-$ s^{-1} on a planar Ni-NTA functionalized electrode, suggesting the photocurrent may be improved significantly [60]. Mesoporous ITO has also been used in conjunction with a cyt *c*-PSI-based system, resulting in a J_{photo} of ~150 μA cm^{-2} and a PS-I TOF of 35 e$^-$ s^{-1} [22]. Despite the large gains, the best EQEs have only approached 17%, indicating the majority of incident light is still not absorbed [24•] and that more PC loading is required.

Multi-layer assembly

One strategy to further increase the loading of RCs on electrodes includes the immobilization of multiple layers. Stieger *et al.* [48•] used alternating deposition of positively charged PSI-cyt *c* complexes with negatively charged DNA to obtain a J_{photo} of 25 μA cm^{-2}, with a PS-I TOF of 21 e$^-$ s^{-1}. Ciesielksi *et al.* [34] used vacuum-assisted solvent evaporation to adsorb a thick multilayer film of PS-I on gold, resulting in peak photocurrent densities (J_{peak}) ~8 μA cm^{-2} which stabilized at 2 μA cm^{-2}. Ravi *et al.* [40••] employed solubilized RC-LH1 in a tandem biophotoelectrode, leading to J_{peak} ~60 μA cm^{-2} which stabilized at ~9 μA cm^{-2}. Most significantly, the work showed the potential for employing genetically modified RC-LH1 to expand the spectral range of the biophotoelectrodes. While these strategies are attractive for increasing the total loading and spectral range of RCs, the increasing EQE is typically undermined by decreasing IQE, as electron transfer to increasingly distal redox active sites becomes hampered.

One strategy to further increase the loading of RCs on electrodes includes encapsulation in a polymer hydrogel. An earlier study immobilized BRCs in an Al_2O_3 sol–gel resulting in photocurrent densities of approximately 5 μA cm^{-2} [61]. However, photocurrents were relatively small for the large quantity of RCs[1], because they were limited by mass transport of the soluble electron donor (sodium dithionite) through the gel and a high rate of charge recombination. These electron transfer limitations in multilayer systems may be resolved with addition of redox centers, akin to the cytochrome electron relays in monolayer configurations. Badura *et al.* [46] was one of the first to implement this strategy with RCs, by mixing PS-II in an osmium–redox hydrogel[2] and obtaining J_{photo} 45 μA cm^{-2}. Kothe *et al.* [23•] embedded PS-I in the same osmium–redox polymer and, by exploiting pH-dependent properties of the poly(vinyl)imidazole backbone, optimized electron transfer rates through the gel to obtain a J_{photo} of 322 μA cm^{-2} (λ = 685 nm at 40 mW cm^{-2}). Most significantly, the TOF of the PS-I was estimated to be larger than PS-I TOF *in vivo*, at 335 e$^-$ s^{-1} vs. 47 e$^-$ s^{-1} *in vivo*, which is the highest reported turnover frequency for PS-I in a biophotoelectrode to date. Satisfying the fast turnover rate while simultaneously loading multiple layers of RCs overcomes two of the long-standing bottlenecks in biophotovoltaic performance. However, the capture of the high reducing power of PS-I without loss to oxygen or other charge recombination mechanisms remains a challenge.

A particularly strong element of the redox hydrogel is the capacity to tune the reduction potential, enabling band alignment of the redox polymer to that of the RCs for higher V_{OC}. This was shown in the work of Plumeré *et al.* [62•] in a tandem PS-I/PS-II electrode with hydrogels that were matched to the donor and acceptor sites of the PS-I and PS-II, respectively, resulting in an increase in the V_{OC} from 90 mV [63] to 372 mV [62•].

Combining the high loading capacity of ultrahigh surface area electrodes with fast electron transfer and multilayer connectivity of redox polymers tackles the problem of obtaining high EQE and TOF simultaneously. This has been investigated with PS-II embedded in a redox polymer on a mesoporous inverse-opal ITO electrode to obtain photocurrents via DET on the order of 410 μA cm^{-2} and a reported TOF of ~15 e$^-$ s^{-1} PSII^{-1} (λ = 685 nm at 10 mW cm^{-2}) [21••]. The addition of the hydrogel enabled the integration of the PS-II into the host material, eliminating the drawbacks of mediated electron transfer, and resulted in a high faradaic efficiency (current to oxygen) of 85 ± 9%, the highest to date. While the peak photocurrent is lower than the previously reported value of 1300 μA cm^{-2} via MET [24•], DET was only 20 μA cm^{-2} in the earlier configuration. The combination of nanostructured electrodes and redox polymers is yet to be shown with PS-I and bacterial RC-based systems and

[1] From their reported film OD of 0.05 we estimated Γ_{RC} = 122 pmol cm^{-2}.

[2] Osmium(byp)$_2$Cl modified poly(vinyl)imidazol.

represents the current benchmark of biophotoelectrode performance.

Solid state electrodes

The diffusion limited mass transport of the mediator bridging the gap between the cathode and anode may become the ultimate bottleneck in biophotovoltaics. Using the design principles of organic photovoltaics, Das *et al.* circumvented diffusional limitations via a solid state configuration (Au|Ni-NTA|RC|C_{60}|bathocruproine|Ag)[3] to obtain a J_{photo} of ~120 μA cm^{-2} [33] and a V_{OC} of 0.025 V, albeit under very high light intensity (λ = 808 nm at 10,000 mW cm^{-2}). Gordiichuk *et al.* [39] explored this solid state configuration further with an ITO|TiO_2|PS-I|PTAA|MoO_3/Al configuration, whereby PS-I was embedded in a PTAA[4] conductive polymer. This yielded a low J_{SC} 0.3 μA cm^{-2} but an unprecedented V_{OC} of 0.76 V thanks to suitable band alignment of selected materials.

Photoactive semiconductor substrates such as titanium dioxide (TiO_2), zinc oxide (ZnO), or hematite (Fe_2O_3) are often used as a substrate upon which the RCs are immobilized. Ocakoglu *et al.* [44] immobilized PS-I multilayers on hematite, obtaining J_{photo} of ~50 μA cm^{-2} and a V_{OC} of 0.321 V. Mershin *et al.* [31] immobilized PS-I on TiO_2 to obtain 362 μA cm^{-2} and a V_{OC} of 0.5 V, with a power conversion efficiency of η = 0.08%. Shah *et al.* [25] electro-sprayed PS-I on a TiO_2 substrate to obtain 4.15 mA cm^{-2}, the highest photocurrent to date for any biophotoelectrode. However, this was obtained in a half-cell configuration under bias utilizing not only mediated but sacrificial electron donors. While these represent the highest performing biophotoelectrodes, these biohybrid-semiconductor-based systems vastly underperform relative to the current dye-sensitized or perovskite solar cells upon which they are based, which reach photocurrent densities on the order of tens of mA cm^{-2} and V_{OC}'s ~0.6 V, and η approaching 20% (NREL).

Concluding remarks

Perhaps one of the most underemphasized limitations for biophotovoltaic applications is the low durability of photosynthetic pigment-proteins, which in their native environment are constantly being replaced. One of the first targets is to decipher the origin and effect of generated reactive oxygen species, which are deleterious to both the photocurrent magnitude via competing charge transfer pathways, and pigment-protein stability [64]. Hydro-gels retain a large percentage of water (80% w/v) which helps to preserve the natural protein conformation after film-drying [23•]. A peptide detergent has also been shown to stabilize BRCs and PS-I under desiccation in the work of Das *et al.* [33] and Mershin *et al.* [31], respectively.

While PSII-based systems have obtained some of the highest performing biophotoelectrodes in terms of photocurrents, the highest turnover numbers per RC (TON) over the entire lifetime of the cell only approach ~16,000 e$^-$ PSII^{-1} [21••]. Conversely, BRC-based systems have exceeded 1 million TON under constant 1-sun illumination on a bare metal electrode [20••], attesting to their relative robustness.

While most biophotoelectrodes have shown stability on the order of hours, Gizzie *et al.* [35•] reported a solid-state Ag/PS-I:polyaniline/TiO_2 with a stability exceeding 3 × 12 h alternations of light on and off, while exhibiting a moderate photocurrent density of 72 μA cm^{-2}. This represents the highest known PSI stability to date and holds promise for improved PS-I stability via a solid state configuration.

Unfortunately, without high-resolution wavelength-dependent EQE plots, the precise role of PCs on photoactive substrates in studies on TiO_2 are difficult to disentangle, as an intact PS-I spectrum is not always clear [31]. One solution in such instances is to measure the photocurrent under far red (>600 nm) illumination to isolate the photocurrent contribution from the PCs and not TiO_2 sensitized by chlorophylls, as shown previously [65].

Due to the inherently small cross-section of a single photosynthetic complex coupled with limitations in electron tunneling distances, high surface area electrodes for high loading combined with fast and long-range electronic connectivity are essential for obtaining substantial photocurrent densities. Coupling this with the highly retained potential energy of the RC via tunable redox materials is essential to obtain high power conversion efficiencies. Circumventing the diffusion limited mass transport may be overcome with a solid state configuration, via a second tuned redox polymer or electron acceptor film as shown in Das *et al.* [33], all while preventing looming charge recombination [66•]. In contrast with works aiming at improved photocurrent densities, the diagnostic tools of protein-film photoelectrochemistry and other biophysical methods are becoming increasingly important for defining electron transfer pathways. This is key for developing strategies to overcome electron transfer bottlenecks and charge recombination pathways and increasing the onset potentials [29•,67,43]. For example, Zhang *et al.* [66•] demonstrated that a PSII-fullerene matrix led to undesirable short-circuits of the PS-II water-oxidation pathway. Friebe *et al.* [43•] improved RC-biophotocathode onset potentials and photocurrents by characterizing and optimizing the cyt *c* electron transfer conditions. Perhaps the most underutilized methods for making bio-

[3] C_{60} = fullerene electron acceptor, bathocuproine/Ag = top electrode.

[4] PTAA = polytriarylamine polymer, a hole transport layer, MoO_3/Al = a common top electrode in OPVs.

photoelectrodes is the toolkit of protein engineering itself: to modulate the delicate photosynthetic protein into a robust biophotovoltaic protein by optimizing redox midpoint potentials, self-assembly [68], broadened spectral range [40••] and more.

References and recommended reading

Papers of particular interest, published within the period of review, have been highlighted as:

- • Paper of special interest.
- •• Paper of outstanding interest.

1. Moore GF, Brudvig GW: **Energy conversion in photosynthesis: a paradigm for solar fuel production**. *Annu Rev Condens Matter Phys* 2011, **2**(2):303–327. http://dx.doi.org/10.1146/annurev-conmatphys-062910-140503.

2. Ringsmuth AK, Landsberg MJ, Hankamer B: **Can photosynthesis enable a global transition from fossil fuels to solar fuels, to mitigate climate change and fuel-supply limitations?** *Renewable Sustainable Energy Rev* 2016, **62**:134–163. http://dx.doi.org/10.1016/j.rser.2016.04.016.

3. Ort DR, Merchant SS, Alric J, Barkan A, Blankenship RE, Bock R, Croce R, Hanson MR, Hibberd JM, Long SP, et al.: **Redesigning photosynthesis to sustainably meet global food and bioenergy demand**. *Proc Natl Acad Sci USA* 2015, **112**:8529–8536. http://dx.doi.org/10.1073/pnas.1424031112.

4. Cogdell RJ, Gardiner AT, Molina PI, Cronin L: **The use and misuse of photosynthesis in the quest for novel methods to harness solar energy to make fuel**. *Philos Trans R Soc A*, vol 371 2013 20110603. http://dx.doi.org/10.1098/rsta.2011.0603.

5. Renger G, Sopory SK, Singhal GS, Irrgang K-D, Govindjee: *Introduction to Photobiology, Photosynthesis and Photomorphogenesis*. Netherlands: Springer; 1999. http://dx.doi.org/10.1007/978-94-011-4832-0_1.

6. Sener M, Strumpfer J, Singharoy A, Hunter CN, Schulten K: **Overall energy conversion efficiency of a photosynthetic vesicle**. *eLIFE*, vol 5 2016. http://dx.doi.org/10.7554/eLife.09541.

7. van Grondelle R, van Gorkom H: **The birth of the photosynthetic reaction center: the story of Lou Duysens**. *Photosynth Res* 2014, **120**:3–7. http://dx.doi.org/10.1007/s11120-013-9959-2.

8. Jones MR: **The petite purple photosynthetic powerpack**. *Biochem Soc Trans* 2009, **37**:400–407. http://dx.doi.org/10.1042/BST0370400.

9. Maróti P, Wraight CA: **The redox midpoint potential of the primary quinone of reaction centers in chromatophores of *Rhodobacter sphaeroides* is pH independent**. *Eur Biophys J* 2008, **37**:1207–1217. http://dx.doi.org/10.1007/s00249-008-0301-4.

10. Allen JP, Williams JC, Graige MS, Paddock ML, Labahn A, Feher G, Okamura MY: **Free energy dependence of the direct charge recombination from the primary and secondary quinones in reaction centers from *Rhodobacter sphaeroides***. *Photosynth Res* 1998, **55**:227–233. http://dx.doi.org/10.1023/A:1005977901937.

11. Brettel K: **Electron transfer and arrangement of the redox cofactors in photosystem I**. *Biochim Biophys Acta* 1997, **1318**:322–373. http://dx.doi.org/10.1016/S0005-2728(96)00112-0.

12. Moser CC, Dutton PL: **Application of Marcus theory to photosystem I electron transfer**. Photosystem I. Netherlands, Dordrecht: Springer; 2006:583–594. http://dx.doi.org/10.1007/978-1-4020-4256-0_34.

13. Rappaport F, Guergova-Kuras M, Nixon PJ, Diner BA, Lavergne J: **Kinetics and pathways of charge recombination in photosystem II**. *Biochemistry* 2002, **41**:8518–8527. http://dx.doi.org/10.1021/bi025725p.

14. Robinson HH, Crofts AR: **Kinetics of the oxidation-reduction reactions of the photosystem II quinone acceptor complex, and the pathway for deactivation**. *FEBS Lett* 1983, **153**:221–226. http://dx.doi.org/10.1016/0014-5793(83)80152-5.

15. Shockley W, Queisser HJ: **Detailed balance limit of efficiency of *p–n* junction solar cells**. *J Appl Phys* 1961, **32**:510–519. http://dx.doi.org/10.1063/1.1736034.

16. Belghachi A: **Theoretical calculation of the efficiency limit for solar cells**: *Solar Cells–New Approaches and Reviews*. InTech; 2015. http://dx.doi.org/10.5772/58914.

17. Mirvakili SM, Slota JE, Usgaocar AR, Mahmoudzadeh A, Jun D, Mirvakili MN, Beatty JT, Madden JDW: **Photoactive electrodes incorporating electrosprayed bacterial reaction centers**. *Adv Funct Mater* 2014, **24**:4789–4794. http://dx.doi.org/10.1002/adfm.201400350.

18. Ravi SK, Tan SC: **Progress and perspectives in exploiting photosynthetic biomolecules for solar energy harnessing**. *Energy Environ Sci* 2015, **8**:2551–2573. http://dx.doi.org/10.1039/C5EE01361E.

19. Yehezkeli O, Tel-Vered R, Michaeli D, Willner I, Nechushtai R: **Photosynthetic reaction center-functionalized electrodes for photo-bioelectrochemical cells**. *Photosynth Res* 2014, **120**:71–85. http://dx.doi.org/10.1007/s11120-013-9796-3.

20. •• Friebe VM, Delgado JD, Swainsbury DJK, Gruber JM, Chanaewa A, Van Grondelle R, Von Hauff E, Millo D, Jones MR, Frese RN: **Plasmon-enhanced photocurrent of photosynthetic pigment proteins on nanoporous silver**. *Adv Funct Mater* 2016, **26**:285–292. http://dx.doi.org/10.1002/adfm.201504020.
Reaction center light harvesting-1 complex (RC-LH1) were adsorbed onto a mesoporous silver electrode, increasing RC-LH1 loading and photocurrent density relative to a planar control. Fluorescence spectroscopy and wavelength dependent external quantum efficiency show a plasmonic enhancement by the silver nanostructure of the RC-LH1 light harvesting efficiency 2.5-*fold*.

21. •• Sokol K, Mersch D, Hartmann V, Zhang JZ, Nowaczyk MM, Roegner M, Ruff A, Schuhmann W, Plumere N, Reisner E: **Rational wiring of photosystem II to hierarchical indium tin oxide electrodes using redox polymers**. *Energy Environ Sci* 2016, **16**:1027–1033. http://dx.doi.org/10.1039/C6EE01363E.
Multilayer immobilization of Photosystem-II in a conductive phenothiazine-modified polymer were combined with an ultrahigh surface area electrode, inverse-opal mesoporous ITO. The combination led to a high performance, fully integrated PS-II electrode system with high protein loading and faradaic efficiency.

22. Stieger KR, Feifel SC, Lokstein H, Hejazi M, Zouni A, Lisdat F: **Biohybrid architectures for efficient light-to-current conversion based on photosystem I within scalable 3D mesoporous electrodes**. *J Mater Chem A* 2016, **4**:17009–17017. http://dx.doi.org/10.1039/C6TA07141D.

23. • Kothe T, Pöller S, Zhao F, Fortgang P, Rögner M, Schuhmann W, Plumeré N: **Engineered electron-transfer chain in photosystem 1 based photocathodes outperforms electron-transfer rates in natural photosynthesis**. *Chemistry* 2014, **20**:11029–11034. http://dx.doi.org/10.1002/chem.201402585.
By refining a redox hydrogel film for maximum electron-transfer rates, the authors demonstrated PS-I turnover frequency that outperformed PSI in vivo. This resulted in large photocurrent densities over 300 μA cm−2, the largest to date for a non-photoactive planar substrate.

24. • Mersch D, Lee CY, Zhang JZ, Brinkert K, Fontecilla-Camps JC, Rutherford AW, Reisner E: **Wiring of photosystem II to hydrogenase for photoelectrochemical water splitting**. *J Am Chem Soc* 2015, **137**:8541–8549. http://dx.doi.org/10.1021/jacs.5b03737.
By wiring Photosystem-II and hydrogenase to separate hierarchical ITO electrodes, the authors revealed a tandem cell that couples PS-II water splitting with hydrogen evolution from hydrogenase via the flow of electrons in an external circuit. The hierarchical mesoporous ITO electrode enabled massive PS-II loading, and resulted in record photocurrent densities that exceeded 1 mA cm−2.

25. Shah VB, Henson WR, Chadha TS, Lakin G, Liu H, Blankenship RE, Biswas P: **Linker-free deposition and adhesion of photosystem i onto nanostructured TiO_2 for biohybrid photoelectrochemical cells**. *Langmuir* 2015, **31**:1675–1682. http://dx.doi.org/10.1021/la503776b.

26. Nguyen K, Bruce BD: **Growing green electricity: progress and strategies for use of photosystem I for sustainable photovoltaic energy conversion**. *Biochim Biophys Acta* 2014, **1837**:1553–1566. http://dx.doi.org/10.1016/j.bbabio.2013.12.013.

27. Kato M, Zhang JZ, Paul N, Reisner E: **Protein film photoelectrochemistry of the water oxidation enzyme photosystem II**. *Chem Soc Rev* 2014, **43**:6485. http://dx.doi.org/10.1039/C4CS00031E.

28. Badura A, Kothe T, Schuhmann W, Rögner M: **Wiring photosynthetic enzymes to electrodes**. *Energy Environ Sci* 2011, **4**:3263. http://dx.doi.org/10.1039/c1ee01285a.

29. • Plumeré N, Nowaczyk MM: **Biophotoelectrochemistry of photosynthetic proteins**. Advances in Biochemical Engineering Biotechnology; 2016:127–141. http://dx.doi.org/10.1007/10_2016_7.
This work is an indispensable guide for understanding and constructing biophotovoltaic devices and biophotoelectrochemical cells. Furthermore, it outlines the standard characterizations and conditions that should be adopted when reporting biophotoelectrode performance.

30. Simmerman RF, Zhu T, Baker DR, Wang L, Mishra SR, Lundgren CA, Bruce BD: **Engineering photosystem I complexes with metal oxide binding peptides for bioelectronic applications**. *Bioconjugate Chem* 2015, **26**:2097–2105. http://dx.doi.org/10.1021/acs.bioconjchem.5b00374.

31. Mershin A, Matsumoto K, Kaiser L, Yu D, Vaughn M, Nazeeruddin MK, Bruce BD, Graetzel M, Zhang S: **Self-assembled photosystem-I biophotovoltaics on nanostructured $TiO_{(2)}$ and ZnO**. *Sci Rep* 2012, **2**:234. http://dx.doi.org/10.1038/srep00234.

32. Trammell SA, Wang L, Zullo JM, Shashidhar R, Lebedev N: **Orientated binding of photosynthetic reaction centers on gold using Ni-NTA self-assembled monolayers**. *Biosens Bioelectron* 2004, **19**:1649–1655. http://dx.doi.org/10.1016/j.bios.2003.12.034.

33. Das R, Kiley PJ, Segal M, Norville J, Yu AA, Wang L, Trammell SA, Reddick LE, Kumar R, Stellacci F, et al.: **Integration of photosynthetic protein molecular complexes in solid-state electronic devices**. *Nano Lett* 2004, **4**:1079–1083. http://dx.doi.org/10.1021/nl049579f.

34. Ciesielski PN, Faulkner CJ, Irwin MT, Gregory JM, Tolk NH, Cliffel DE, Jennings GK: **Enhanced photocurrent production by photosystem I multilayer assemblies**. *Adv Funct Mater* 2010, **20**:4048–4054. http://dx.doi.org/10.1002/adfm.201001193.

35. • Gizzie EA, Scott Niezgoda J, Robinson MT, Harris AG, Jennings GK, Rosenthal SJ, Cliffel DE: **Photosystem I-polyaniline/TiO_2 solid-state solar cells: simple devices for biohybrid solar energy conversion**. *Energy Environ Sci* 2015, **8**:3572–3576. http://dx.doi.org/10.1039/C5EE03008K.
PSI integrated in a conductive polyaniline polymer on a titanium dioxide anode, topped off with a silver cathode to form a solid-state PSI biophotovoltaic device. The device had a remarkable open circuit voltage around 0.35 V, and a photocurrent density $\sim$72 μA cm−2. Most significantly the device had a remarkably durability under 3 × 12 h of alternating illumination over 3 days.

36. Suemori Y, Fujii K, Ogawa M, Nakamura Y, Shinohara K, Nakagawa K, Nagata M, Iida K, Dewa T, Yamashita K, Nango M: **Molecular assembly of artificial photosynthetic antenna core complex on an amino-terminated ITO electrode**. *Colloids Surf B* 2007, **56**:182–187. http://dx.doi.org/10.1016/j.colsurfb.2006.10.029.

37. Kondo M, Nakamura Y, Fujii K, Nagata M, Suemori Y, Dewa T, Iida K, Gardiner AT, Cogdell RJ, Nango M: **Self-assembled monolayer of light-harvesting core complexes from photosynthetic bacteria on a gold electrode modified with alkanethiols**. *Biomacromolecules* 2007, **8**:2457–2463. http://dx.doi.org/10.1021/bm070352z.

38. Kondo M, Iida K, Dewa T, Tanaka H, Ogawa T, Nagashima S, Nagashima KVP, Shimada K, Hashimoto H, Gardiner AT, Cogdell RJ, Nango M: **Photocurrent and electronic activities of oriented-his-tagged photosynthetic light-harvesting/reaction center core complexes assembled onto a gold electrode**. *Biomacromolecules* 2012, **13**:432–438. http://dx.doi.org/10.1021/bm201457s.

39. Gordiichuk PI, Wetzelaer GJAH, Rimmerman D, Gruszka A, De Vries JW, Saller M, Gautier DA, Catarci S, Pesce D, Richter S, Blom PWM, Herrmann A: **Solid-state biophotovoltaic cells containing photosystem I**. *Adv Mater* 2014, **26**:4863–4869. http://dx.doi.org/10.1002/adma.201401135.

40. •• Ravi SK, Yu Z, Swainsbury DJK, Ouyang J, Jones MR, Tan SC: **Enhanced output from biohybrid photoelectrochemical transparent tandem cells integrating photosynthetic proteins genetically modified for expanded solar energy harvesting**. *Adv Energy Mater* 2017, **7**:1–7. http://dx.doi.org/10.1002/aenm.201601821.
The authors constructed a tandem-biophotoelectrode utilizing two modified RC-LH1 complexes in a solution on PEDOT:PSS coated conductive glass. The two RC-LH1 complexes had a modified complimentary spectral range leading to an increased absorption range, and is one of the first instances where protein engineering is shown to lead to improved biophotoelectrode performance.

41. Den Hollander MJ, Magis JG, Fuchsenberger P, Aartsma TJ, Jones MR, Frese RN: **Enhanced photocurrent generation by photosynthetic bacterial reaction centers through molecular relays, light-harvesting complexes, and direct protein-gold interactions**. *Langmuir* 2011, **27**:10282–10294. http://dx.doi.org/10.1021/la2013528.

42. Kamran M, Delgado JD, Friebe V, Aartsma TJ, Frese RN: **Photosynthetic protein complexes as bio-photovoltaic building blocks retaining a high internal quantum efficiency**. *Biomacromolecules* 2014, **15**:2833–2838. http://dx.doi.org/10.1021/bm500585s.

43. • Friebe VM, Millo D, Swainsbury DJK, Jones MR, Frese RN: **Cytochrome *c* provides an electron-funneling antenna for efficient photocurrent generation in a reaction center biophotocathode**. *ACS Appl Mater Interfaces* 2017 acsami.7b03278. http://dx.doi.org/10.1021/acsami.7b03278.
The powerful tool of protein-film voltammetry in conjunction with photoelectrochemistry is utilized to investigate the cyt c mediated electron transfer architecture of a RC-LH1-cyt c electrode. The cyt c film was optimized to improve the onset potential of the cyt c electron transfer relay and increase photocurrents on a functionalized mesoporous silver electrode up to $\sim$100 μA cm−2.

44. Ocakoglu K, Krupnik T, van den Bosch B, Harputlu E, Gullo MP, Olmos JDJ, Yildirimcan S, Gupta RK, Yakuphanoglu F, Barbieri A, Reek JNH, Kargul J: **Photosystem I-based biophotovoltaics on nanostructured hematite**. *Adv Funct Mater* 2014, **24**:7467–7477. http://dx.doi.org/10.1002/adfm.201401399.

45. Kato M, Cardona T, Rutherford AW, Reisner E: **Covalent immobilization of oriented photosystem II on a nanostructured electrode for solar water oxidation**. *J Am Chem Soc* 2013, **135**:10610–10613. http://dx.doi.org/10.1021/ja404699h.

46. Badura A, Guschin D, Esper B, Kothe T, Neugebauer S, Schuhmann W, Rögner M: **Photo-induced electron transfer between photosystem 2 via cross-linked redox hydrogels**. *Electroanalysis* 2008, **20**:1043–1047. http://dx.doi.org/10.1002/elan.200804191.

47. Feifel SC, Stieger KR, Lokstein H, Lux H, Lisdat F: **High photocurrent generation by photosystem I on artificial interfaces composed of π-system-modified graphene**. *J Mater Chem A* 2015, **3**:12188–12196. http://dx.doi.org/10.1039/C5TA00656B.

48. • Stieger KR, Ciornii D, Kölsch A, Hejazi M, Lokstein H, Feifel SC, Zouni A, Lisdat F: **Engineering of supramolecular photoactive protein architectures: the defined co-assembly of photosystem I and cytochrome c using a nanoscaled DNA-matrix**. *Nanoscale* 2016, **8**:10695–10705. http://dx.doi.org/10.1039/C6NR00097E.
A self-assembling conductive multilayer system composed entirely out of biologically derived components—Photosystem-I, cyt c and DNA was developed. The cyt c provided a conductive network, while the negatively charged DNA bound together the positively charged PSI-cyt c domains electrostatically, resulting in photorrent densities up to 25 μA cm−2.

49. Lebedev N, Trammell SA, Spano A, Lukashev E, Griva I, Schnur J: **Conductive wiring of immobilized photosynthetic reaction center to electrode by cytochrome *c***. *J Am Chem Soc* 2006, **128**:12044–12045. http://dx.doi.org/10.1021/ja063367y.

50. Trammell SA, Griva I, Spano A, Tsoi S, Tender LM, Schnur J, Lebedev N: **Effects of distance and driving force on photoinduced electron transfer between photosynthetic reaction centers and gold Electrodes**. *J Phys Chem C* 2007, **111**:17122–17130. http://dx.doi.org/10.1021/jp0740402.

51. Yaghoubi H, Li Z, Jun D, Lafalce E, Jiang X, Schlaf R, Beatty JT, Takshi A: **Hybrid wiring of the *Rhodobacter sphaeroides* reaction center for applications in bio-photoelectrochemical solar cells**. *J Phys Chem C* 2014, **118**:23509–23518. http://dx.doi.org/10.1021/jp507065u.

52. Yaghoubi H, Lafalce E, Jun D, Jiang X, Beatty JT, Takshi A: **Large photocurrent response and external quantum efficiency in biophotoelectrochemical cells incorporating reaction center plus light harvesting complexes**. *Biomacromolecules* 2015, **16**:1112–1118. http://dx.doi.org/10.1021/bm501772x.

53. Yaghoubi H, Schaefer M, Yaghoubi S, Jun D, Schlaf R, Beatty JT, Takshi A: **A ZnO nanowire bio-hybrid solar cell**. *Nanotechnology* 2017, **28**:54006. http://dx.doi.org/10.1088/1361-6528/28/5/054006.

54. Zhao J, Zou Y, Liu B, Xu C, Kong J: **Differentiating the orientations of photosynthetic reaction centers on Au electrodes linked by different bifunctional reagents**. *Biosens Bioelectron* 2002, **17**:711–718. http://dx.doi.org/10.1016/S0956-5663(02)00026-X.

55. Lu Y, Yuan M, Liu Y, Tu B, Xu C, Liu B, Zhao D, Kong J: **Photoelectric performance of bacteria photosynthetic proteins entrapped on tailored mesoporous WO_3-TiO_2 films**. *Langmuir* 2005, **21**:4071–4076. http://dx.doi.org/10.1021/la0470129.

56. Millo D, Ranieri A, Gross P, Ly HK, Borsari M, Hildebrandt P, Wuite GJL, Gooijer C, van der Zwan G: **Electrochemical response of cytochrome *c* immobilized on smooth and roughened silver and gold surfaces chemically modified with 11-mercaptounodecanoic acid**. *J Phys Chem C* 2009, **113**:2861–2866. http://dx.doi.org/10.1021/jp807855y.

57. Kamran M, Delgado JD, Friebe V, Aartsma TJ, Frese RN: **Photosynthetic protein complexes as bio-photovoltaic building blocks retaining a high internal quantum efficiency**. *Biomacromolecules* 2014, **15**:2833–2838. http://dx.doi.org/10.1021/bm500585s.

58. Gebert J, Reiner-Rozman C, Steininger C, Nedelkovski V, Nowak C, Wraight CA, Naumann RLC: **Electron transfer to light-activated photosynthetic reaction centers from *Rhodobacter sphaeroides* reconstituted in a biomimetic membrane system**. *J Phys Chem C* 2015, **119**:890–895. http://dx.doi.org/10.1021/jp510006n.

59. Kato M, Cardona T, Rutherford AW, Reisner E: **Photoelectrochemical water oxidation with photosystem II integrated in a mesoporous indium-tin oxide electrode**. *J Am Chem Soc* 2012, **134**:8332–8335. http://dx.doi.org/10.1021/ja301488d.

60. Badura A, Esper B, Ataka K, Grunwald C, Wöll C, Kuhlmann J, Heberle J, Rögner M: **Light-driven water splitting for (bio-)hydrogen production: photosystem 2 as the central part of a bioelectrochemical device**. *Photochem Photobiol* 2006, **82**:1385–1390. http://dx.doi.org/10.1562/2006-07-14-RC-969.

61. Zhao J, Ma N, Liu B, Zhou Y, Xu C, Kong J: **Photoelectrochemistry of photosynthetic reaction centers embedded in Al_2O_3 gel**. *J Photochem Photobiol A* 2002, **152**:53–60. http://dx.doi.org/10.1016/S1010-6030(02)00188-0.

62. Hartmann V, Kothe T, Pöller S, El-Mohsnawy E, Nowaczyk MM, Plumeré N, Schuhmann W, Rögner M: **Redox hydrogels with adjusted redox potential for improved efficiency in Z-scheme inspired biophotovoltaic cells**. *Phys Chem Chem Phys* 2014, **16**:11936–11941. http://dx.doi.org/10.1039/C4CP00380B.

63. Kothe T, Plumeré N, Badura A, Nowaczyk MM, Guschin DA, Rögner M, Schuhmann W: **Combination of a photosystem 1-based photocathode and a photosystem 2-based photoanode to a Z-scheme mimic for biophotovoltaic applications**. *Angew Chem Int Ed* 2013, **52**:14233–14236. http://dx.doi.org/10.1002/anie.201303671.

64. Nowaczyk MM, Plumeré N: **Photosynthesis: Short circuit at the chlorophyll**. *Nat Chem Biol* 2016, **12**:990–991. http://dx.doi.org/10.1038/nchembio.2240.

65. Amunts A, Toporik H, Borovikova A, Nelson N: **Structure determination and improved model of plant photosystem I**. *J Biol Chem* 2010, **285**:3478–3486. http://dx.doi.org/10.1074/jbc.M109.072645.

66. • Zhang JZ, Sokol KP, Paul N, Romero E, van Grondelle R, Reisner E: **Competing charge transfer pathways at the photosystem II-electrode interface**. *Nat Chem Biol* 2016, **12**:1046–1052. http://dx.doi.org/10.1038/nchembio.2192.
Protein-film electrochemistry of a PSII-fullerene-ITO electrode was used to identify a charge transfer pathway that was short-circuiting the known water-oxidation pathway, resulting in undesirable O2 reduction.

67. Friebe VM, Swainsbury DJK, Fyfe PK, van der Heijden W, Jones MR, Frese RN: **On the mechanism of ubiquinone mediated photocurrent generation by a reaction center based photocathode**. *Biochim Biophys Acta* 2016, **1857**:1925–1934. http://dx.doi.org/10.1016/j.bbabio.2016.09.011.

68. Swainsbury DJK, Harniman RL, Di Bartolo ND, Liu J, Harper WFM, Corrie AS, Jones MR: **Directed assembly of defined oligomeric photosynthetic reaction centres through adaptation with programmable extra-membrane coiled-coil interfaces**. *Biochim Biophys Acta* 2016, **1857**:1829–1839. http://dx.doi.org/10.1016/j.bbabio.2016.09.002.